genesis 50:86–101 (2012)

ARTICLE

DNApol-ε Gene Is Indispensable for the Survival and Growth of *Drosophila melanogaster*

Akanksha Verma, Sonali Sengupta, and Subhash C. Lakhotia*

Department of Zoology, Cytogenetics Laboratory, Banaras Hindu University, Varanasi, India

Received 1 July 2011; Revised 12 August 2011; Accepted 14 August 2011

Summary: Based on deletion and complementation mapping and DNA sequencing, a new recessive fully penetrant mutation (*DNApol-ε^{pl10R}*), causing prolonged larval life and larval/early pupal lethality, is identified as the first mutant allele of the *DNApol-ε* (*CG6768*) gene of *Drosophila melanogaster*. A same-sense base pair substitution in exon 1 of the *DNApol-ε* gene is associated with retention of the first intron and significant reduction in DNApol-ε transcripts in *DNApol-ε^{pl10R}* homozygotes. Homozygous mutant larvae show small imaginal discs with fewer cells and reduced polyteny in salivary glands, presumably because of the compromised DNA polymerase function following exhaustion of the maternal contribution. Extremely small and rare *DNApol-ε^{pl10R}* homozygous somatic clones in *DNApol-ε^{pl10R}/+* imaginal discs confirm their poor mitotic activity. The *DNApol-ε^{pl10R}* homozygotes, like those expressing *DNApol-ε-RNAi* transgene, show high sensitivity to DNA damaging agents. The first mutant allele of the *DNApol-ε* gene will facilitate functional characterization of this enzyme in the genetically tractable *Drosophila* model. genesis 50:86–101, 2012. © 2011 Wiley Periodicals, Inc.

Key words: DNA polymerase epsilon; splicing defect; hsr-omega; Hrp36; *pl10R*; DNA damage

INTRODUCTION

Transmission of genetic information requires genome duplications by high fidelity DNA polymerases. Eukaryotes possess five major DNA polymerases, viz., α, β, γ, ε, and δ, of which the DNA polymerase ε (DNApol-ε) is one of the major leading strand DNA synthesis enzyme; the DNApol-ε is also implicated in DNA repair, recombination, and chromatin organization (Araki *et al*., 1992; Budd and Campbell, 1993; Morrison *et al*., 1990; Nishida *et al*., 1988; Pursel and Kunkel, 2008; Zlotkin *et al*., 1996). DNApol-ε isolated from *Drosophila melanogaster* embryos (dPol-ε) has polymerase and proofreading activity similar to its homologs in other organisms (Aoyagi *et al*., 1997). Sequence comparison revealed a 40.9% amino acid sequence identity of dPol-ε with the human and 22.9% with *Saccharomyces cerevisiae* DNApol-ε (Oshige *et al*., 2000), suggesting functional similarity with the DNApol-ε of other eukaryotes. However, a functional analysis of *DNApol-ε* (*CG6768*) gene has been limited by the non-availability of any mutant allele in *D. melanogaster*. In this report, we characterize the first loss of function recessive mutant allele of *Pol-ε* which leads to severe growth retardation and lethality at late larval/early pupal stages.

In an earlier report from our laboratory, it was suggested that the P-transposon insertion in the *hsrω^{05241}* chromosome was responsible for their recessive male sterility (Rajendra *et al*., 2001). With a view to confirm this, crosses were setup at that time to mobilize the P-transposon inserted at −130 bp position in the *hsrω^{05241}* chromosome. Some progeny in these crosses exhibited a recessive larval-pupal lethality along with the continued presence of the P-transposon and recessive

Additional Supporting Information may be found in the online version of this article.

Current address for Sonali Sengupta: School of Biosciences and Technology, VIT University, Vellore, India.

*Correspondence to: Subhash C. Lakhotia, Department of Zoology, Cytogenetics Laboratory, Banaras Hindu University, Varanasi 221005, India.

E-mail: lakhotia@bhu.ac.in

Contract grant sponsors: Department of Science and Technology (DST), Government of India, New Delhi (to S.C.L.), University Grants Commission, New Delhi, and the Indian Council of Medical Research (New Delhi) (to A.V.), Council of Scientific and Industrial Research, New Delhi (to S.S.).

Published online 26 August 2011 in
Wiley Online Library (wileyonlinelibrary.com).

DOI: 10.1002/dvg.20791

male sterility. Other subsequent studies in our laboratory (Akanksha *et al*., 2008) revealed that the male sterility initially ascribed by Rajendra *et al*. (2001) to the P-transposon insertion in the *hsrω*^{05241} chromosome was erroneous since the male sterility was actually due to a second site mutation in a cytoplasmic dynein intermediate chain gene in the 61B cytogenetic region. Likewise, the new larval-pupal lethal phenotype seen in progeny following the crosses for mobilization of the P-transposon in *hsrω*^{05241} allele was also found to be due to a second site mutation, which was named as *l(3)pl10*^{R} (Sengupta, 2005; also see Materials and Methods). In the present study, we describe effects of this mutation on development and differentiation of larval and imaginal tissues and characterize the *l(3)pl10*^{R} mutant allele genetically and molecularly. Our results suggest that the *l(3)pl10*^{R} mutation carries a single base substitution in the first exon of the *DNAPol-ε* gene (*CG6768*; available at: http://flybase.org) which affects splicing of the first intron and causes loss of DNAPol-ε activity. Accordingly, we have renamed the *l(3)pl10*^{R} mutation as *DNApol-ε*^{pl10R} and the same is referred to in the text here as *pl10R*.

RESULTS

Homozygosity for *pl10R* Mutation Causes Late Larval/Early Pupal Death

The *pl10R* homozygous embryos hatch normally and initially develop like their heterozygous sibs (*pl10R/TM6B*). However, with the beginning of third instar stage they begin to show developmental and other defects. Early to mid third instar *pl10R* homozygous larvae gradually become akinetic and persist as thin larvae for several days (Fig. 1a,a′). The puparia formed by *pl10R* homozygous larvae are abnormal, being markedly narrower and elongated (Fig. 1b,b′). All *pl10R* homozygous progeny die, as late larvae/early pupae, about 12 days after hatching from egg. The *pl10R* mutant larvae often show presence of small melanotic patches (Fig. 1a′). The *pl10R/TM6B* or *pl10R/+* larvae are indistinguishable from wild-type larvae and develop normally under standard rearing conditions.

Cell Growth and Proliferation are Affected in *pl10R* Homozygous Mutants

The 6-day-old *pl10R* homozygous mutant larvae show remarkable differences in growth of endoreplicating as well as mitotically dividing imaginal cells from those in 6-day-old wild-type or *pl10R/TM6B* larvae (Fig. 1). All imaginal discs and the brain ganglia in 6- or 9-day-old *pl10R* larvae are very small, like those in second instar wild-type larvae (Fig. 1c–e′); the discs are misshapen and thus difficulty in identification. Salivary glands (SG) of 6- or 9-day-old *pl10R* mutant larvae are also very small in size (Fig. 1f′,f”). Double staining of SGs of wild-type and 6- or 9-day-old *pl10R* larvae with DAPI and the cell membrane specific protein Armadillo (Riggleman *et al*., 1990) revealed that while the number of endoreplicated cells is same in wild-type and the *pl10R* mutant glands (data not presented), the individual cells in SGs of *pl10R* homozygous larvae are much smaller than in wild type (Fig. 1g,g′). Interestingly, compared with wild type (Fig. 1h), the number of the diploid imaginal cells in SG ducts is significantly reduced in the *pl10R* homozygous larvae (Fig. 1h′).

Unlike SGs, the overall dimensions of gut and the endoreplicated cells therein are generally comparable in 6-day-old homozygous *pl10R* and wild-type larvae (Fig. 1i,i′). However, the gut imaginal cells, present as clusters of small cells interspersed between the endoreplicated larval gut cells, are fewer in the mutant larvae. Each such cluster in the mid gut region shows about 7 to 10 cells in the *pl10R* homozygotes rather than 18 to 20 imaginal cells in wild-type gut (Fig. 1i,i′).

Immunostaining of wing discs with Armadillo ab (Fig. 1j,j′) reveals that while the cell size in the mutant and wild-type discs is comparable, the mutant discs carry fewer cells. Immunostaining of leg (Fig. 1c,c′) and wing discs (Fig. 1d,d′) with Wg ab shows that the characteristic wild-type pattern of distribution of the Wingless protein is partly affected in the mis-shaped and smaller discs in mutant larvae. Thus, while the Wg staining around the wing pouch and the DV margin in the mutant wing discs is present in a distorted manner, the notum region is much more affected. Immunostaining of eye discs with the mab22C10, which identifies the neuronal cells (Fujita *et al*., 1982), shows that unlike in wild-type eye discs (Fig. 1k), ommatidial units in 6- (Fig. 1k′) or 9-day-old (Fig. 1k”) *pl10R* larvae are completely absent.

Expression of the Nuclear Transcript of *hsrω* in *pl10R* Cells is Altered

Dig-labeled antisense riboprobe corresponding to the repeat region of the *hsrω* gene (Prasanth *et al*., 2000) was hybridized in situ to RNA in intact or partially squashed brain ganglia or Malpighian tubules (MT) from normally grown wild-type or *pl10R* homozygous larvae. As reported earlier (Lakhotia *et al*., 1999, Prasanth *et al*., 2000), hsrω-n RNA is distributed in wild-type MT nuclei as many (150–200) fine nucleoplasmic omega speckles along with a strong signal at a single chromatin site, the site of transcription (Fig. 1l). However, in many of the 6- or 9-day-old *pl10R* mutant MT cells, the speckled pattern is replaced by variable numbers of large clusters or aggregates (Fig. 1l′); the site of transcription also shows a stronger signal than in wild-type MT cells. Based on the numbers of speckles and their sizes, the different MT cells from the

pl10R mutant larvae are categorized into the following four patterns:

- Pattern I—the wild-type MT pattern (Fig. 11,l′).
- Pattern II—a bigger cluster of hsrω-n RNA at the site of transcription and fewer (50–70) but often clustered omega speckles (Fig. 11′).
- Pattern III—still fewer (30–50) omega speckles and a greater accumulation of transcripts at the site of transcription (Fig. 11′).
- Pattern IV—signal intensity at the site of transcription is very high with very few or no nucleoplasmic omega speckles or their clusters (Fig. 11′).

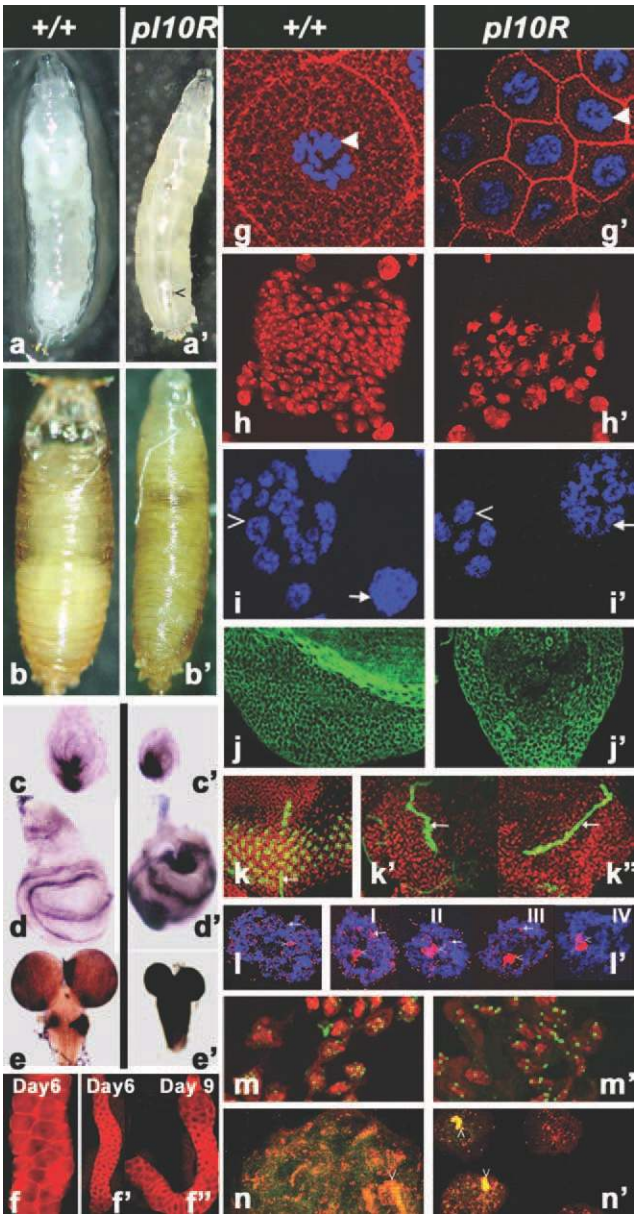

Data on relative frequencies of these different patterns of hsrω-n RNA distribution in wild-type and *pl10R* mutant MT cells are presented in Figure 2. All wild-type MT cells show the fine omega speckles (Pattern I), but in *pl10R* mutant MT cells, this pattern is seen in less than 5% cells. Most of the cells from both 6- as well as 9-day-old mutant larvae show Type II or III pattern. Significantly, MT nuclei from 9-day-old *pl10R* larvae show increasing incidence of Types III and IV patterns (Fig. 2).

Colorimetric detection of the hsrω-n RNA in intact brain ganglia of 6-day-old larvae shows that the much smaller brain and ventral ganglia from the mutant larvae have significantly higher levels of the hsrω-n transcripts (Fig. 1d,d′). FRISH on partially squashed brain ganglia cells reveals that compared with the presence of 8 to 10 omega speckles/nucleus in wild-type unstressed brain cells (Fig. 1m), the *pl10R* brain cells show only one or two larger cluster/s of hsrω-n transcripts (Fig. 1m′).

Distribution of hnRNP is Also Altered in *pl10R* Mutant Cells in Parallel With hsrω-n RNA

Fluorescence RNA-RNA in situ hybridization followed by immunostaining with the P11 antibody, which stains

FIG. 1. Diverse effects of *pl10R* mutation on larval morphology and internal structures. In each paired panels (**a–n** and **a′–n′**, respectively), images from wild type (+/+) larvae are shown on left (a–n) while the corresponding images at same magnifications from *pl10R* homozygous larvae are on the right (a′–n′). a–a′ Six- and 9-day-old larvae; b–b′ early brown pupae. c–d and c′–d′ Prothoracic leg (c, c′) and wing (d–d′) imaginal discs from 6-day-old larvae immunostained with anti–Wg ab. e–e′ Brain ganglia complexes following RNA:RNA in situ hybridization followed by chromogenic detection of hsrω-n transcripts; f–f′ and f″ confocal sections of intact SG from 6-day-old +/+ (f) and 6- (f′) or 9-day-old (f″) *pl10R* homozygous larvae immunostained with anti-Armadillo ab. g–g′ Distal SG cells from 6-day-old larvae stained with DAPI (blue) and anti-Armadillo ab (red). h–h′ Confocal projection images of DAPI stained intact SG ducts to show the imaginal SG nuclei from 6-day-old wild-type (h) and *pl10R* (h′) larvae. i–i′ Confocal sections of DAPI-stained midgut region of 6-day-old larvae showing large polytene nuclei (arrows) and groups of imaginal histoblasts (arrowheads); j–j′ Confocal sections of wing imaginal discs from 6-day-old larvae, immunostained with anti-Armadillo ab. k, k′–k″ Confocal sections of eye discs from 6-day-old wild-type (k) or 6- (k′) or 9-day-old (k″) *pl10R* larvae immunostained with mab22C10, which recognizes the differentiated photoreceptor cells and Bolwig's nerve (green). l–l′ Confocal sections of MT principle cells from 6-day-old larvae following FRISH to detect the hsrω-n transcripts (red); arrowheads point to the site of *hsrω* gene transcription while arrows point to nucleoplasmic omega speckles; l′ shows the patterns I–IV of omega speckles in principle cells of *pl10R* larvae (see text for details; the DAPI stained chromatin is blue). m–m′ Confocal sections of lightly squashed brain ganglia cells from 6-day-old wild-type (m) or 9-day-old *pl10R* (m′) larvae following FRISH to detect the hsrω-n transcripts (green); DAPI stained chromatin is in red. n–n′ Merged images of confocal sections of SG of 6-day-old wild-type (n) or *pl10R* homozygous (n′) larvae after FRISH to detect the hsrω-n transcripts (green), and immunostaining with the P11 ab to localize Hrp36 protein (red); their colocalization sites appear yellow; arrowheads point to the *hsrω* gene site where the hsrω-n transcripts and Hrp36 are aggregated.

the Hrp36 hnRNP, was carried out in intact SGs from wild-type and *pl10R* mutant larvae. Unlike the earlier reported (Lakhotia *et al*., 1999; Prasanth *et al*., 2000) fine pattern in wild-type cells (Fig. 1n), the hsrω-n RNA in the mutant SG cells is seen as clusters/aggregates with one big cluster at the chromatin site of transcription (Fig. 1n′). The Hrp36 protein colocalizes with the clusters of hsrω-n RNA in nucleoplasm and at the site of transcription (see Fig. 1n–n′). Similarly altered distribution of hnRNPs and hsrω-n transcripts is seen in other cell types also (not shown).

Cells of *pl10R* Mutants are not Stressed

The clustered distribution of hsrω-n transcript and omega speckles in cells of *pl10R* homozygous mutants is reminiscent of heat shocked wild-type cells (Lakhotia *et al*., 1999; Prasanth *et al*., 2000). Therefore, to see if cells of *pl10R* homozygous larvae are under some kind of cellular stress, the SGs of normally developing 6- or 9-day-old wild-type and *pl10R* larvae, respectively, were immunostained with stress-induced Hsp70-specific 7Fb antibody (Velasquez and Lindquist, 1984). Immunostaining of control tissues from 24°C grown larvae shows that the Hsp70 protein is completely absent in wild-type (Fig. 3a) as well as in *pl10R* cells (Fig. 3b). As a positive control, SGs of wild-type and *pl10R* homozygous mutants were heat shocked at 37°C for 40 min and immunostained with the 7Fb antibody. As shown in Figure 3c,d, Hsp70 is present both in the cytoplasm and nucleus of wild type as well as *pl10R* homozygous mutants after 40 min of heat shock. This indicates that cells of *pl10R* mutant larvae which show aggregated omega speckles are not stressed but are competent to show stress induced synthesis of Hsp70.

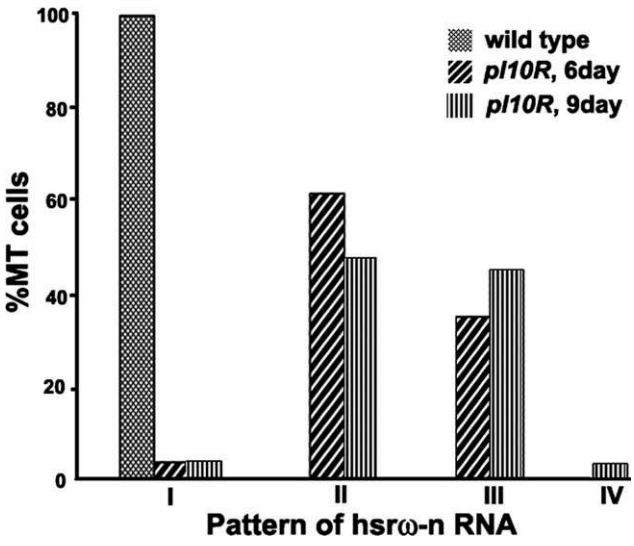

FIG. 2. Histograms of the frequency of different patterns (I–IV) of hsrω-n distribution in MT nuclei of wild-type and *pl10R* third instar larvae.

Poor Mitotic Activity/Survival of *pl10R* Homozygous Cells is Autonomous in Mitotic Clones

In order to know if the slow growth associated with this mutation is cell autonomous, somatic clones were generated using the FLP-FRT system (Golic and Lindquist, 1989; Xu and Rubin, 1993) with GFP as marker for clones resulting from somatic recombination. The *y w; hs-FLP; P[ry*$^+$ *t7.2 = neoFRT]82B pl10R/P[ry*$^+$ *t7.2 = neoFRT]82B Ubi-GFP pl10R*$^+$ first instar larvae were heat shocked for 1 h at 37°C and allowed to develop at 24°C to third instar larval stage. A total of 54 imaginal discs from these larvae were examined for the presence of twin spots of GFP-null (*pl10R/pl10R* homozygous) and GFP-bright *GFP pl10R*$^+$*/GFP pl10R*$^+$cells amidst GFP dull *GFP pl10R*$^+$*/pl10R* heterozygous background. A total of 39 clones (+/+) with intense GFP fluorescence amidst GFP-dull *GFP pl10R*$^+$*/pl10R* heterozygous cells were identified. Intriguingly, however, only five of them had the associated GFP null (*pl10R/pl10R*) clones. Interestingly, compared with the large number of the GFP bright cells in each of these five clones, the

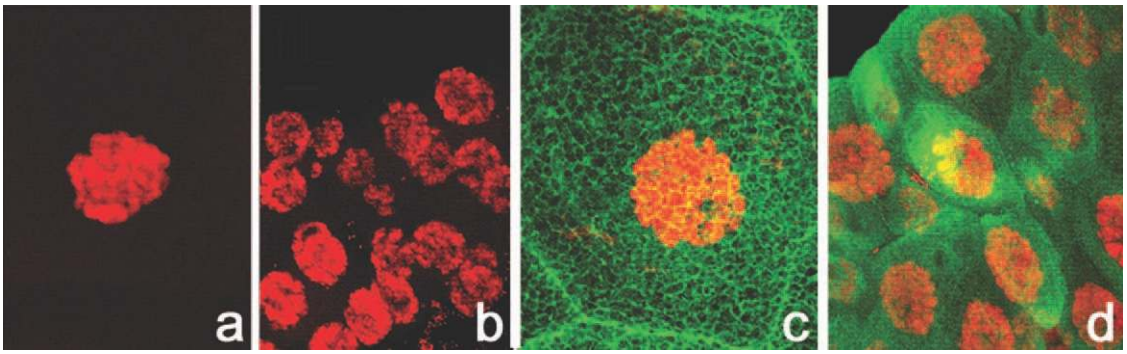

FIG. 3. Hsp70 is absent in larval SG cells of wild-type and *pl10R* third instar larvae under control conditions (**a, b**) but is induced after a 40 min heat shock at 37°C (**c, d**). a and c are wild-type while b and d are *pl10R* SG cells under control and heat shock conditions, respectively. DAPI-stained chromatin is red and Hsp70 is green.

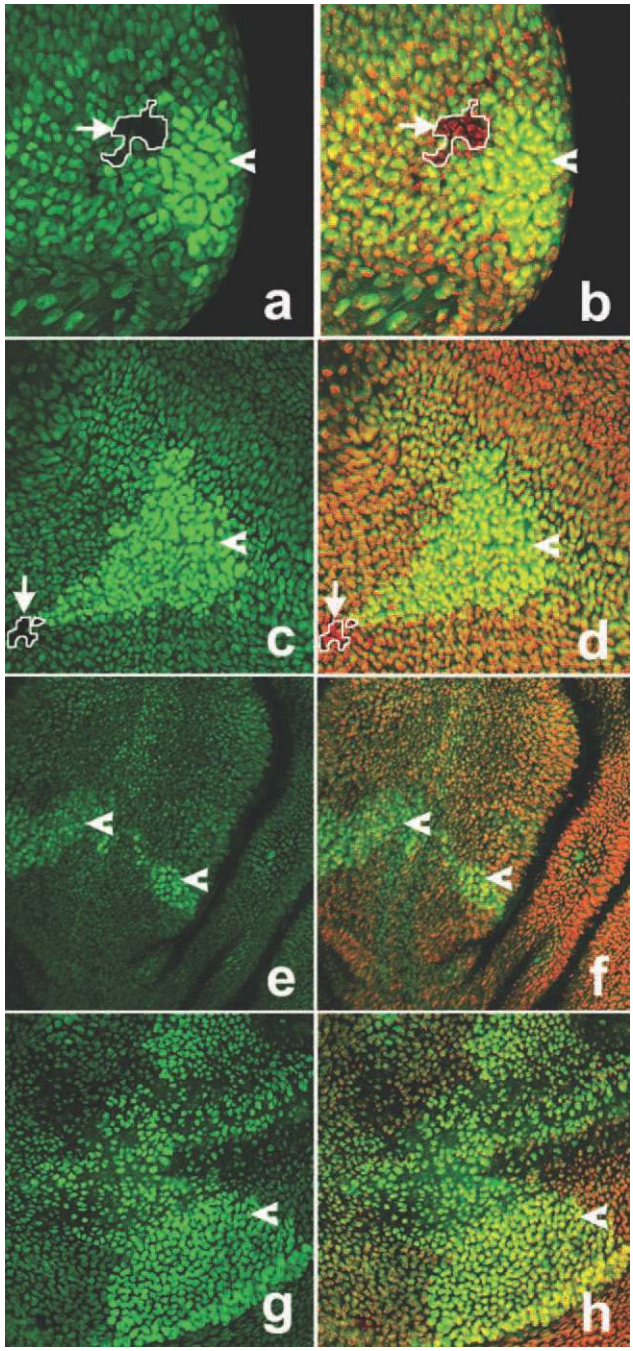

FIG. 4. Confocal images of *pl10R* homozygous mutant and +/+ twin spots in *hs-FLP;+/+; pl10R FRT-82B/FRT-82B-Ubi-GFP* $pl10R^{+}$ eye (**a**, **b**), wing (**c**–**f**), or leg (**g**, **h**) imaginal discs from late third instar larvae that were heat shocked at the first instar stage. The *pl10R*/+ cells show dull nuclear GFP fluorescence while the +/+ cells in mosaic clones show more intense green fluorescence (arrowheads). Compared to the extensive GFP bright +/+ clones, the *pl10R*/*pl10R* (GFP null) clones are either very small (arrows and encircled areas) consisting of only a few cells visible in the DAPI (in red) stained images (b, d) or are completely absent (f, h).

GFP-null clones were much smaller, with only three to four cells (Fig. 4).

Rarity of the *pl10R* homozygous clones and the much smaller number of cells in those present, suggests that the *pl10R/pl10R* mutant cells are very slow dividing and/or have poor viability.

Genetic, Deletion, and Complementation Mapping Suggest the *pl10R* Mutation to Affect the *DNApol-ε* (*CG6768*) Gene

Recombination mapping of the *pl10R* mutation using the multiply marked *ru cu ca* chromosome 3 (Lindsley and Zimm, 1992) suggested the *pl10R* mutation to map at 78.39 cM on chromosome 3 (data not presented), which corresponds to the 94A-95F cytogenetic region on polytene chromosomes maps (Lindslay and Zimm, 1992). Deletion mapping with a series of third chromosomal deficiency lines (Fig. 5) spanning the cytological interval from 93E to 95A3 was carried out to further refine the location. Among the larger deficiencies, only the *Df(3R)M95A*, with deletion of the 94D to 95A3 cytological interval (available at: www.flybase.org), fails to complement the *pl10R* mutation. In order to further narrow down the location of *pl10R* mutation, a set of smaller Exelixis deficiencies (shown as grey bars in the middle panel of Fig. 5) spanning the region from 93B to 96A13 was used. The *pl10R* mutation complements all of these smaller deficiencies (see Supporting Information Table S1; the breakpoints of the various Exelixis deficiencies are as given in Release 3 available at: www.flybase.org). Proximal and distal limits of *pl10R* mutation is thus defined by the distal breakpoint (19,162,766 bp) of the *Df(3R)Exe19012* and the proximal break point (19,201,551 bp) of the *Df(3R)Exe16194* chromosomes (Drysdale *et al*., 2005). The 39 kb region in the 94E13-94F1 interval, accordingly, remained uncovered and, therefore, the *pl10R* mutation is putatively placed in this 39kb region (Fig. 5).

The Flybase (available at: www.flybase.org) lists eight genes, viz. *pnt*, *Sec13*, *RpS3*, *DNApol-ε (Polε)*, *ATP-SynCF6*, *CG4408*, *CG42827*, and *CG42828* (*CG6784*) in the 39 kb region of the 94E13-94F1 cytological interval (Fig. 5). *P*-element insertion mutant alleles of five of these genes, viz., $pnt^{KG04968}$ and $P\{PZ\}pnt^{07825}$ for *pnt*; $P(PZ)sec13^{01031}$ for *Sec13*, $RpS3^{Plac92}$ for *RpS3*, $P\{EPgy2\}ATPsyn\text{-}Cf6^{EY22484}$ for *ATP-SynCF6*, and $PBac\{WH\}CG6784^{f01032}$ for *CG42828* (*CG6784*) (see at: www.flybase.org for details of the different alleles) fully complement the *pl10R* phenotype. *Act-GAL4* driven expression of *CG4408-RNAi* transgene (*4408-R3* from NIG Fly) also does not exhibit any phenotype, neither by itself (+; *Act-GAL4*/+; *CG4408-RNAi*/+) nor in the *pl10R* background (+; *Act-GAL4*/+; *CG4408-RNAi*/*pl10R*).

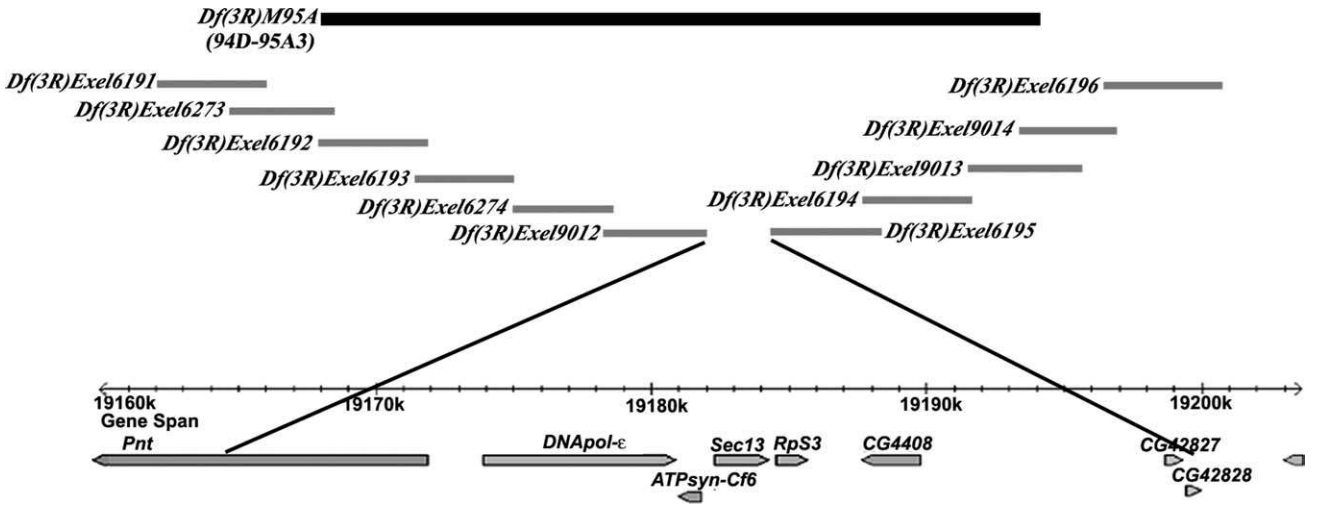

FIG. 5. Diagrammatic representation of the various Exelixis deletion chromosomes (grey bars), that overlap with or flank the *Df(3R)M95A* (black bar on top) and were used for mapping the *pl10R* mutation. The grey bars, corresponding to the deleted region in the given chromosomes, are positioned relative to the genomic scale shown in the middle (with base numbers as in Release 3.0, available at: www.flybase.org). Other Exelixis deletion chromosomes, with deletions beyond the far right side of the *M95A* deletion were also used but are not shown in this figure (see Supp. Info., Table S1). Organization and orientation of the eight genes *pnt*, *DNApol-ε*, *ATPsyn-CF6*, *sec13*, *RpS3*, *CG4408, CG42827*, and *CG42828* (*CG6784*) in the 39kb region of the cytological interval 94E13-94F1 are shown in the lower part (adapted from www.flybase.org) with the pointed end indicating the direction of transcription of each gene.

Table 1
pl10R Mutation Enhances Pupal Lethality due to Act5C-GAL4 Driven Global Expression of Polε-RNAi Transgene

Crosses	Total eggs	No. eggs hatched	Third instar larvae transferred	Pupae formed	Flies eclosed	
					Genotype/s	Number/s
[a]*Act5C-GAL4/CyO*; +/+ X *Act5C-GAL4/CyO*; +/+ (*Act5C-GAL4* and *CyO* homozygotes die as embryo or early larvae)	805	610 (*O* = 75.7) (*E* = 75)	375 (*O* = 46.6) (*E* = 50)	373 (*O* = 46.3) (*E* = 50.0)	*Act5C-GAL4/CyO*; +/+	371 (*O* = 46) (*E* = 50)
pl10R/TM6B X +/+	330	330 (*O* = 100) (*E* = 100)	328 (*O* = 99.4) (*E* = 100)	328 (*O* = 99.4) (*E* = 100)	*TM6B*/+	162 (*O* = 49.1) (*E* = 50)
					pl10R/+	158 (*O* = 47.9) (*E* = 50)
[a]*Act5C-GAL4/CyO*; +/+ X *Polε-RNAi/CyO*;+/+ (*CyO* homozygotes die as embryo or early larvae)	860	620 (*O* = 72.1) (*E* =.75)	613 (*O* = 71.3) (*E* = 75)	601 (*O* = 69.9) (*E* = 75)	*Act5C-GAL4/CyO*; +/+ OR. *Polε-RNAi /CyO*; +/+	413 (*O* = 48) (*E* = 50)
					***Act5C-GAL4/ Polε-RNAi*; +/+**	**99 (*O* = 11.5) (*E* = 25)**
[a]*Act5C-GAL4/CyO; pl10R/ TM6B* X *Polε-RNAi/CyO*;+/ + (*CyO* homozygotes die as embryo or early larvae)	989	716 (*O* = 72.4) (*E* = 75)	637 (*O* = 64.4) (*E* = 75)	617 (*O* = 62.4) (*E* = 75)	*Act5C-GAL4/CyO; TM6B*/+ OR. *Polε-RNAi /CyO; TM6B*/+	244 (*O* = **24.7**) (*E* = 25)
					Act5C-GAL4/CyO; pl10R/+ OR. *Polε-RNAi /CyO; pl10R*/+	234 (*O* = 23.7) (*E* = 25)
					***Act5C-GAL4/ Polε-RNAi; TM6B*/+**	**73 (*O* = 7.4) (*E* = 12.5)**
					***Act5C-GAL4/ Polε-RNAi; pl10R*/+**	**29 (*O* = 2.9) (*E* = 12.5)**

Numbers in parentheses indicate the % observed (*O*) and expected (*E*) values (out of the total number of eggs in column 2). Genotypes that show significant differences between expected and observed ($P < 0.001$) are shown in bold in the last two columns.
[a]All *CyO/CyO* (~25% of all eggs) progeny die at embryonic stage.

In the absence of any available mutant allele of the *Pol-ε*gene annotated to be in the 39 kb interval, we used the *DNApol-ε-RNAi* (referred to in the text as *Pol-ε-RNAi*) line (*6768-R1* from NIG Fly) to see if down regulation of dPol-ε has a phenotype in the *pl10R* background. As seen from the data in Table 1, *Act5C-GAL4*

driven global expression of one copy of the *Pol-ε-RNAi* transgene resulted in ~50% pre-adult (larval and pupal) lethality in *Act5C-GAL4/Pol-ε-RNAi*; +/+ or *Act5C-GAL4/Pol-ε-RNAi; TM6B*/+ progeny genotypes. Significantly, presence of one copy of *pl10R* mutant allele in *Act5C-GAL4* driven *Pol-ε-RNAi* background (*Act5C-GAL4/Pol-ε-RNAi; pl10R*/+ progeny) resulted in much greater pre-adult lethality so that only ~23% of the expected progeny survived to adulthood. It may be noted that one copy of *pl10R* mutant allele in otherwise wild-type background has no effect on viability and likewise, single copy of undriven *Pol-ε-RNAi* transgene also does not affect viability (Table 1).

Together, our findings that the *pl10R* mutation aggravates the pre-adult lethality due to *Pol-ε-RNAi* expression but complements mutant alleles of the other 6 genes in the above defined 39 kb interval, strongly suggest that the *pl10R* mutation affects the *Pol-ε* gene.

The *CG42827* gene is recently annotated on the Flybase with its function remaining unknown. Since no mutant allele for this gene was available, we could not check its complementation status with *pl10R*.

PCR Mapping and Sequencing of *pl10R* Chromosome

In order to identify the nature and exact location of mutation in the *pl10R* chromosome, the 39 kb genomic DNA in the 94E13 to 94F1 cytogenetic interval defined above was scanned through PCR using overlapping sets of primers (details in Supporting Information Table S2). PCR reactions were carried out with the genomic DNA isolated from *pl10R/pl10R* and *hsr*ω^{05241}/*hsr*ω^{05241} homozygous larvae. The *hsr*ω^{05241}/*hsr*ω^{05241} genomic DNA was used as the "wild type" reference for the sequence of the 39 kb region in the *pl10R* chromosome since the *pl10R* mutation originated in the *hsr*ω^{05241} chromosome (see Materials and Methods; Sengupta, 2005). A general identity in the sizes of PCR amplicons generated with *pl10R* and *hsr*ω^{05241} genomic DNAs with all the primer pairs (not shown) suggested absence of any major unique deletion or insertion in the 39 kb interval in the *pl10R* chromosome. The PCR amplicons generated with *pl10R* as well as *hsr*ω^{05241} genomic DNAs using the primer pair CG4408.2F-CG4408.2R were smaller than expected on the basis of the reference sequence available at the www.flybase.org for the corresponding genomic region.

In order to identify smaller lesions that could be correlated with the *pl10R* phenotype, all the amplicons generated for the 39 kb genomic region in *pl10R* and *hsr*ω^{05241} chromosomes were sequenced and the resulting sequences were compared with each other as well as with the reference sequence available in the database (available at: www.flybase.org) using the Clustalw multiple sequence alignment software (Thompson *et al*., 1994).

Sequencing of the above noted smaller amplicons generated with *pl10R* and *hsr*ω^{05241} genomic DNAs using the primers CG4408.2F-CG4408.2R confirmed a 240 bp (from 19189468 to 19189707nt) deletion in the 5′UTR of *CG4408* gene in the *pl10R* as well as *hsr*ω^{05241} chromosomes. Since this deletion of 240 bp is common to the *pl10R* and *hsr*ω^{05241} genomic DNAs, it does not appear to be responsible for the *pl10R* phenotype.

Several other sites in the 39 kb region sequenced by us show differences in the base sequence with respect to that available in www.flybase.org. However, since, except for one (see below), all the changes are common to the *pl10R* and *hsr*ω^{05241} genomic DNA sequences, they are unlikely to be responsible for the *pl10R* mutation (the genomic DNA sequences obtained in our study are deposited in Genbank database, vide accession numbers *JN600259* for the 38542 nucleotides of the *hsr*ω^{05241} genomic DNA and *JN600258* for 8954 nucleotides of the *DNApol-epsilon*^{pl10R} allele).

Comparison of the genomic DNA sequences for the 39 kb region in *pl10R* and *hsr*ω^{05241} chromosomes reveals only one base difference. This is a single base substitution (T444C) in the exon 1 of *Pol-ε* gene in *pl10R* mutant chromosome (Fig. 6). The corresponding sequence in *hsr*ω^{05241} chromosome was comparable to the reference sequence available at www.flybase.org and that provided by Oshige *et al*. (2000). This substitution mutation does not affect the coding function of the mRNA (Fig. 6). Other base changes in the *Pol-ε* gene which are common to *pl10R* and *hsr*ω^{05241} are listed in Table S3 (Supporting Information). In view of the above results with *Pol-ε-RNAi* and other results presented below, we believe that the single base substitution is responsible for the *pl10R* mutant phenotype.

pl10R Mutants Show Reduced Levels of Pol-ε Transcripts

We compared the levels of dPol-ε transcripts in third instar larvae of different genotypes by semiquantitative RT-PCR, using primers that amplify the 3′ end of dPol-ε transcripts (Fig. 7). Mean intensity of the RT-PCR amplicon in *pl10R* homozygotes is about 57% (lane 2, Fig. 7) of that in wild type (lane 1, Fig. 7) while in larvae expressing one copy of *Pol-ε-RNAi* under *Act-GAL4* driver (lane 4, Fig. 7), the signal is about 75% of the wild type. One copy of *pl10R* mutant allele in *Act-GAL4* driven *Polε-RNAi* (lane 5, Fig. 7) background further reduces levels of these amplicons but the reduction is less than in *pl10R* homozygous tissues (Fig. 7).

Fluorescence RNA:RNA in situ hybridization (FRISH) with DNApol-ε specific riboprobe (corresponding to the 3′ part of the DNApol-ε transcript) in third instar larval tissues of the wild type and *pl10R* (Fig. 8) con-

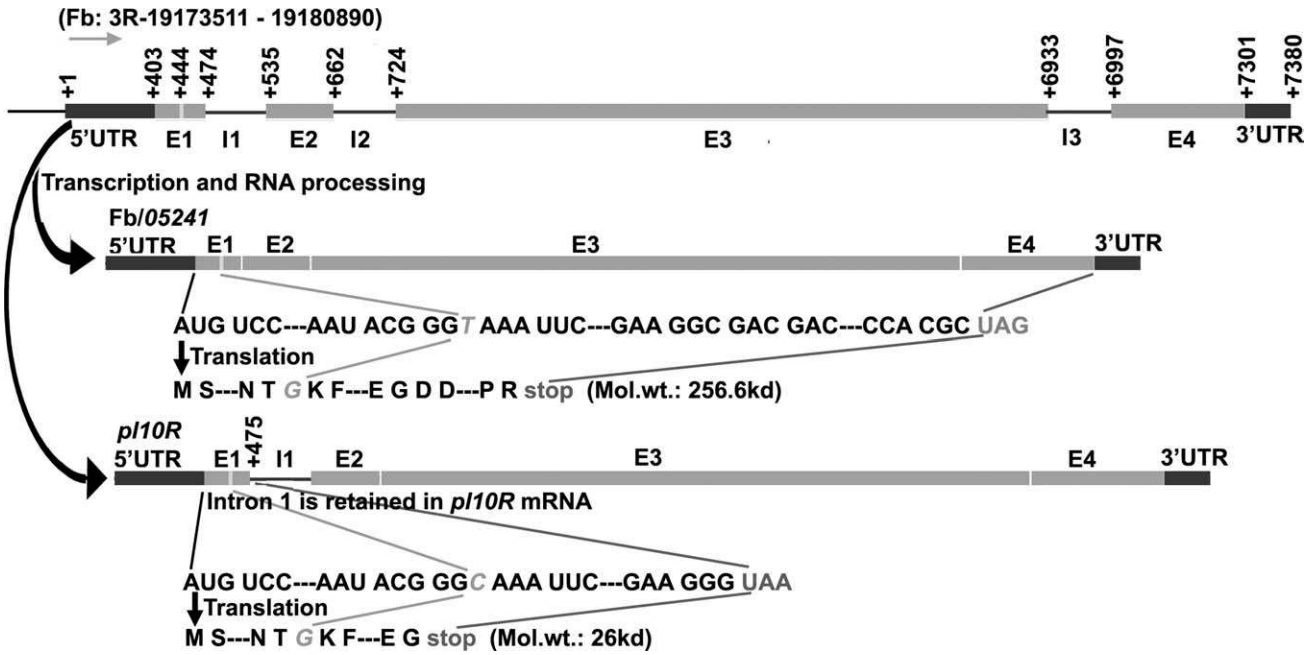

FIG. 6. Architecture of *Pol-ε* gene and its transcript. DNApol-ε transcript is reported by Oshige *et al*. (2000) to have a 402 b 5′ UTR and 80 b 3′ UTR (black boxes) although the annotation available at the www.flybase.org does not indicate the 5′ UTR. The Fb numbers on top indicate the genomic sequence coordinates of the Pol-ε gene as at: www.flybase.org. The grey arrow shows the direction of transcription. The *Pol-ε* gene carries four exons (gray boxes, E1-E4) and three introns (black lines, I1-I3) which are spliced to produce a single transcript (Oshige *et al*., 2000; www.flybase.org). Numbers on the genomic map in top panel indicate locations of transcription start site, the site of mutation in the *pl10R* allele, and the different UTR and exon-intron boundaries. Gray vertical line in the first exon (E1) represents the site of mutation (T444C) in the pl10R allele. The middle panel shows mRNA and partial nucleotide and the translated amino acid sequences in wild type (Fb) and *hsrω*^{05241} (*05241*); the T base at +444 and the corresponding amino acid (G) are indicated in light gray italic letters. The bottom panel shows the transcript in *pl10R* mutants with unspliced intron 1 (see Fig. 9 and text) and the consequent premature translation termination due to the stop codon at +475 position in the retained intron 1; the substituted base C at +444 and the corresponding unchanged amino acid G are shown in light gray italic letters.

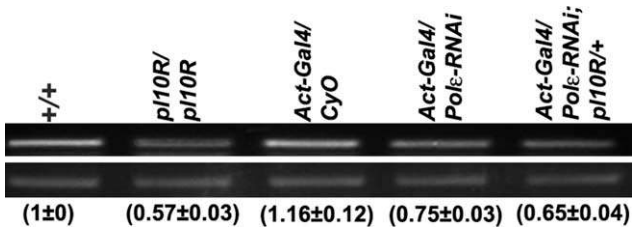

FIG. 7. The *pl10R* mutation reduces level of the DNApol-ε transcripts. Ethidium bromide stained amplicons following semiquantitative RT-PCR of total larval RNA with primer pair DNApol.3F and DNApol.2R (Table 2), specific for exon 3 of DNApol-ε, in different genotypes (mentioned above each lane) are shown in the upper panel. The lower panel shows amplicons obtained with the primer pairs for G3PDH in each sample (loading control). Numerical values in parentheses below each lane indicate the relative mean levels (±SE, $N = 3$), estimated as ratio of fluorescence intensity of the DNA-pol-ε and G3PDH amplicons in the sample, of the DNA-pol-ε transcripts in the given genotype.

firmed the above results. Wild-type imaginal discs (Fig. 8a,c), SGs (Fig. 8e,g), MTs (Fig. 8i), and brain ganglia (Fig. 8k) show high abundance of Pol-ε transcripts in cytoplasm. The mis-shaped imaginal (wing and leg) discs (Fig. 8b,d), SGs with reduced polyteny levels (Fig. 8f,h), MTs (Fig. 8j), and brain ganglia (Fig. 8l) from *pl10R* homozygous larvae display highly reduced levels of Pol-ε transcripts. The hybridization signals in *Act-GAL4/CyO* tissues are comparable to those seen in wild-type tissues (not shown). In parallel with the RT-PCR results noted above, *Act-GAL4* driven *Pol-ε-RNAi* reduces the levels of Pol-ε transcripts in all tissues to some extent while their levels in tissues from *Act-GAL4/Pol-ε*-RNAi; *pl10R/+* larvae are further reduced but not to the same extent as in *pl10R* homozygous larval tissues (not shown).

Splicing of Intron 1 of DNApol-ε Transcript is Affected in *pl10R* Homozygous Larvae

The *Pol-ε* gene is annotated to have three introns (Fig. 6) but only one mRNA product (see available at: www.flybase.org). RT-PCR with primers flanking the three Pol-ε introns was performed to check if the *pl10R* mutation affected splicing. PCR amplification of cDNA from wild type and *pl10R* homozygotes with primers flanking the second and third introns generated amplicons of the expected size (163 bp and 162 bp, respectively, Fig. 9). On the other hand, primers flanking the

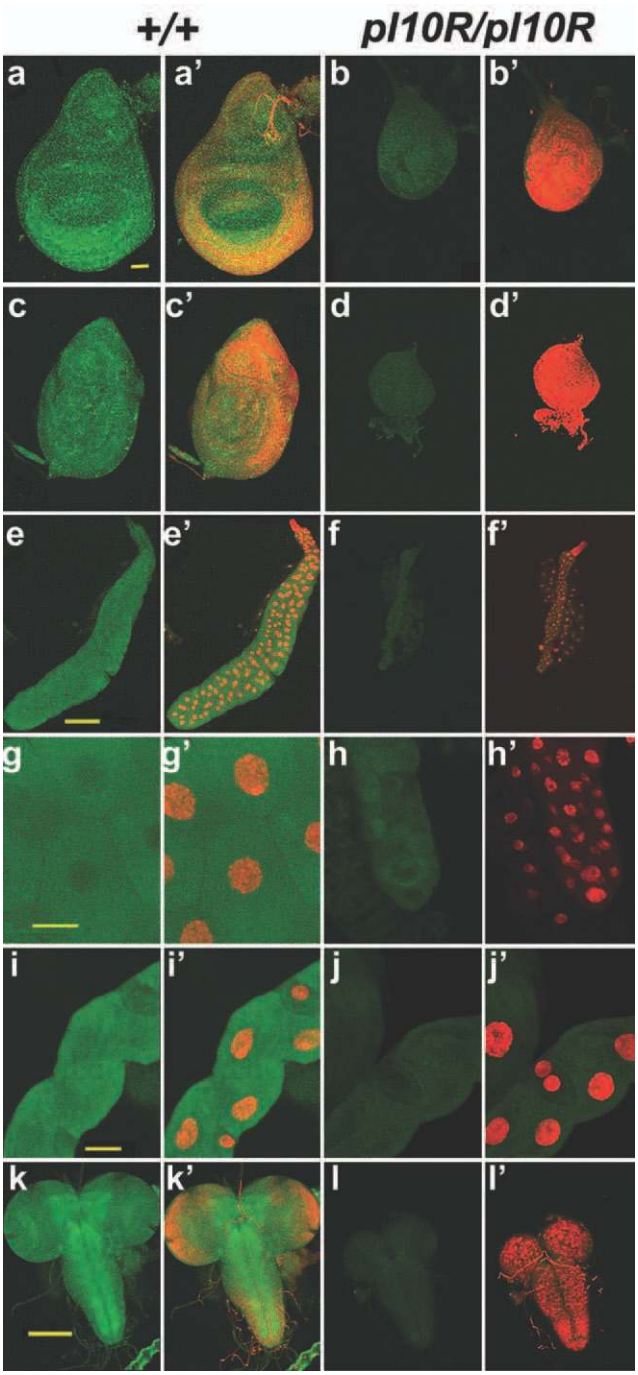

FIG. 8. The *pl10R* mutation reduces DNApol-ε transcripts in wide variety of larval cell types as seen after FRISH with DNApol-ε transcript specific riboprobe (green fluorescence). Confocal projections of whole wing (**a–b**′) and leg (**c–d**′) imaginal discs, salivary glands (**e–f**′), Malpighian tubules (**i–j**′) and brain ganglia (**k–l**′) from larvae of different genotypes (noted on top of columns). **g–h**′ show optical sections of parts of e–f′, respectively, at higher magnification. a–l FRISH images for Pol-ε transcripts (green) while a′–l′ show merged images of Pol-ε transcripts (green) and DAPI-stained chromatin (red). Genotypes are marked on top. The scale bar in a (50 μm) applies to a–d′, in e (200 μm) to e–f′, in g (50 μm) to g–h′, in i (20 μm) to i–j′ and that in k (200 μm) to k–l′.

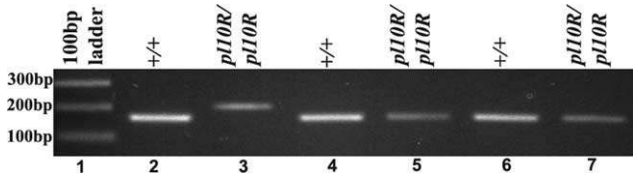

FIG. 9. The first intron of the DNApol-ε is retained in *pl10R* homozygous larval tissues although the second and third introns are normally spliced as revealed by semiquantitative RT-PCR with total RNA from third instar wild-type (lanes 2, 4, and 6) and *pl10R* homozygous (lanes 3, 5, and 7) larvae. Amplicons in lanes 2 and 3 are generated with DNApol-Int1.F and DNApol-Int1.R (flanking intron 1), in lanes 4 and 5 with DNApol-Int2.F and DNApol-Int2.R (flanking intron 2) and in lane 6 and 7 with DNApol-Int3.F and DNApol-Int3.R (flanking intron 3; see Table 2) primer pairs. Molecular size markers are shown in lane 1. The amplicon in lane 3 (*pl10R*) is longer by 60 pairs than in lane 2 (wild type) sample indicating that the intron 1 is not spliced out in *pl10R* mutants.

first intron generate a single amplicon (239 bp, lane 3 of Fig. 9) with the cDNA from *pl10R* third instar larvae which is larger than that obtained with wild-type cDNA (179 bp, lane 2 of Fig. 9). The 60b increase in size of this amplicon from the *pl10R* mutants corresponds with the annotated size (60b) of intron 1.

pl10R Homozygotes are More Sensitive to DNA Damage by Bleomycin

Since the dPol-ε is suggested to be involved in replication as well as in DNA repair (Oshige *et al*., 2004; Pursell and Kunkel, 2008), we examined if the *pl10R* mutation enhances sensitivity to DNA damage using bleomycin, which is known to induce DNA double strand breaks (Povirk *et al*., 1977; 1989). Freshly hatched first instar larvae of various genotypes (Fig. 10) were transferred to food without (control) or with 2.5 μg/ml or 5 μg/ml bleomycin. A dose-dependent early larval death is apparent in all the genotypes fed on bleomycin with *Act-GAL4/Pol-ε-RNAi*; +/+ being more sensitive than wild type or *Act-GAL4/CyO*; +/+ (Fig. 10); the *pl10R* homozygotes are the most sensitive to bleomycin so that most of these larvae die at the first instar stage even with 2.5 μg/ml bleomycin feeding and none of those few which develop to third instar stage pupate (Fig. 10). Interestingly, the adult survivors in the other three genotypes (wild type, *Act-GAL4/CyO*; +/+ and *Act-GAL4/Pol-ε-RNAi*; +/+) appear healthy and fertile.

In view of the above noted higher sensitivity of *pl10R* larvae to bleomycin, we examined chromatin integrity in these mutants by the comet assay. Single cell gel electrophoresis was performed with imaginal disc cells from wild type, *Act-GAL4/CyO*; +/+, *Act-GAL4/Pol-ε-RNAi*; +/+ and +/+; *pl10R/pl10R* third instar larvae grown for 48 hr on normal or bleomycin supplemented (50 μg/ml or 100 μg/ml) food. We compared the proportion of DNA in the comet tail, which is a

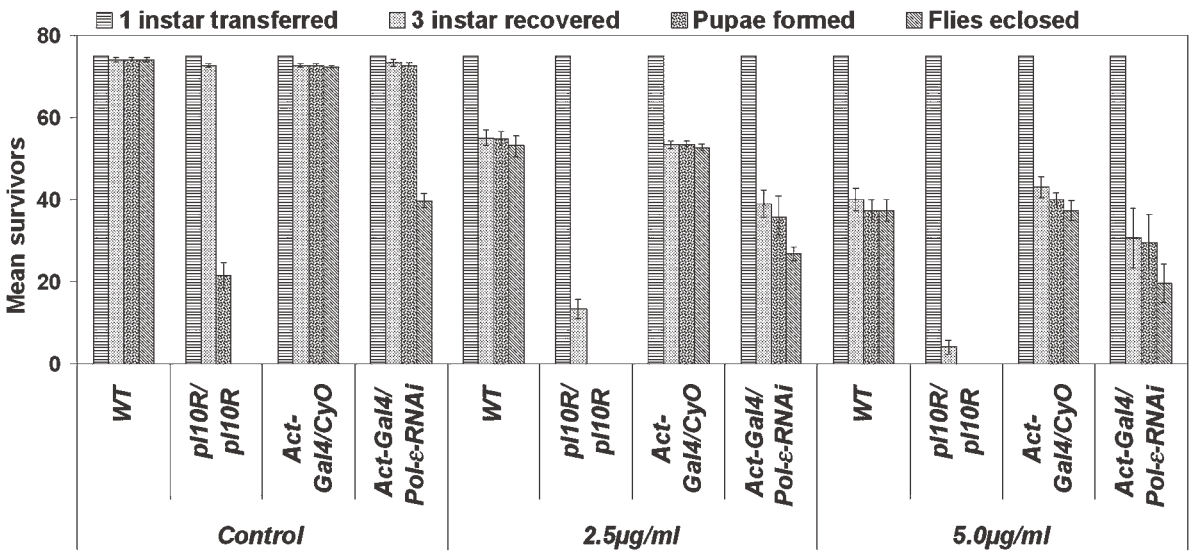

FIG. 10. Bleomycin feeding enhances lethality of *Drosophila* larvae with reduced Pol-ε. Histograms show the mean (±SE, $N = 3$; *y*-axis) numbers of survivors till different developmental stages in different genotypes (*x*-axis) grown on normal or bleomycin-supplemented (2.5 μg/ml or 5 μg/ml) food.

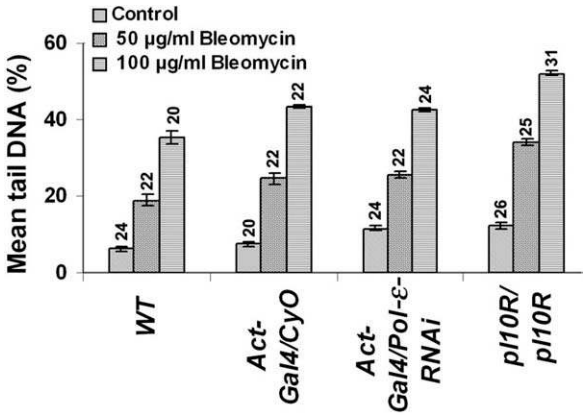

FIG. 11. Comet assay shows a greater proportion of DNA in the comet tail in cells from *pl10R* homozygous larvae grown on normal or bleomycin supplemented (50 μg/ml or 100 μg/ml) food. Histograms show mean (±S.E) % DNA in the comet tail (*y*-axis) in cells from larvae of different genotypes (*x*-axis) grown on normal or bleomycin supplemented food. The number on top of each bar indicates the number of comets analyzed for the given genotype and treatment.

measure of the extent of DNA damage (Kumaravel *et al.*, 2006; Olive, 1999). As seen in Figure 11, the % tail DNA correlates with increasing dose of bleomycin in the larval food. Interestingly, however, compared with wild type the % tail DNA is higher in normally fed *pl10R/pl10R* larvae. The % tail DNA in *Act-GAL4/Pol-ε-RNAi*; +/+ is not significantly different from that in *Act-GAL4/CyO* larvae. Bleomycin feeding causes enhanced DNA damage in all genotypes with the *pl10R* homozygotes showing the highest proportion as tail DNA, reflecting a higher extent of DNA damage (Fig. 11).

DISCUSSION

The diverse phenotypes of the *pl10R* homozygous larvae, like small-sized and malformed imaginal discs, reduced polyteny of SG nuclei, and cessation of growth beyond the early third instar stage, clearly indicate defects in growth and cell division processes. Analysis of twin spots generated by somatic recombination in *pl10R*/+ heterozygous background shows that the poor proliferative potential of *pl10R* homozygous cells is cell autonomous. Cell autonomous phenotype suggests that the growth limitations are unlikely to be due to defects in hormonal signaling. Genetic and deficiency mapping helped us locate this mutation to a 39-kb genomic region which is annotated (available at: www.flybase.org) to harbor eight genes. Six of these, viz., *pnt*, *ATPsyn-CF6*, *sec13*, *RpS3*, *CG4408*, and *CG42828* (*CG6784*) were ruled out by full complementation of the *pl10R* phenotype by mutant alleles of each of them. The *CG42827* gene, newly annotated to be present in this region, does not have any typical mutant allele and the nature of its protein product is also not yet identified (available at: www.flybase.org). However, the *CG42827* gene is unlikely to be affected by the *pl10R* mutation since our DNA sequence of the *CG42827* gene region in the *pl10R* chromosome does not show any change from that in the $hsr\omega^{05241}$ chromosomes.

In view of the slower growth/cell division and reduced polyteny seen in the mutant larvae, the *DNA-*

pol-ε gene appears more likely as the candidate gene affected by the *pl10R* mutation. *DNApol-ε* encodes the catalytic subunit of the DNA polymerase epsilon of *Drosophila melanogaster*. Lack of complementation between *pl10R* and *DNApol-ε-RNAi* transgene expression strongly suggests that the *pl10R* lesion may indeed be affecting the *DNApol-ε* gene. It may be noted that the global activation of one copy of the *DNApol-ε-RNAi* transgene under the *Act5C-GAL4* driver does not result in as strong a phenotype as seen in *pl10R* homozygous larvae yet most of the death following RNAi is during late larval/pupal stages. The milder phenotypes (e.g., lethality, DNA damage, and chromatin integrity) following pol-ε-RNAi may be due to the fact that *Act5C-GAL4* driven expression of one copy of the RNAi transgene reduces the DNApol-ε transcripts only by 25%; in addition, the maternally derived (Oshige *et al*., 2000; Yamaguchi *et al*., 1995) and zygotically synthesized DNApol-ε protein may be more stable so that even after activation of RNAi, the protein remains available. The significant point is that one copy of *pl10R* allele substantially enhances the lethality due to DNApol-ε-RNAi and also causes death at earlier stages than seen with DNApol-ε-RNAi alone.

Further support for our belief that *pl10R* mutation to affects the *DNApol-ε* gene is provided by the findings that (i) the level of DNApol-ε transcripts is substantially reduced in *pl10R* homozygous larval tissues and this is additively further reduced when a single copy of the *DNApol-ε-RNAi* is also expressed and (ii) comparison of the base sequence of the 39 kb genomic DNA in the *pl10R* and its parental $hsr\omega^{05241}$ chromosomes revealed only one base substitution between the two chromosomes and this mapped to exon 1 of the *DNApol-ε* gene.

It is rather surprising that a synonymous base pair substitution in exon 1 of the *DNApol-ε* gene should result in as serious a phenotype as displayed by the *pl10R* homozygous larvae. Intriguingly, our studies revealed severe reduction in DNApol-ε transcripts and retention of the first intron in the *pl10R* mutants. How this single base substitution, which is 29b upstream of the putative first exon-intron splice junction, causes the intron skipping needs additional studies. In silico analysis (data not presented) suggests that though the T444C mutation does not affect the encoded amino acid sequence, it does alter the secondary structure of the Pol-ε precursor RNA. Several studies in different organisms have shown that the secondary structure of primary transcripts can also modulate its accessibility to splicing factors during RNA processing (Chen and Stephan, 2003; Kreahling and Graveley, 2005; Loeb *et al*., 2002; Warf and Berglund, 2009). Since the promoter region of the *DNApol-ε* gene in the *pl10R* chromosome did not show any change in base sequence, we presume that although the transcriptional activity of the mutant allele may not be affected, the significantly reduced cellular levels of the DNApol-ε transcripts in the mutant cells may result from nonsense mediated decay because of the retention of the first intron so that only a small fraction gets transported to cytoplasm as revealed by in situ hybridization. In any case, the persistence of intron 1 would result in premature termination due to the stop codon present in the first intron, leading to greatly truncated protein without the polymerase activity (Fig. 6). Further, since no transcript with normally spliced intron 1 was detectable in the *pl10R* samples by RT-PCR (Fig. 9), it is unlikely that any functional DNApol-ε is produced in the mutant cells.

Rescue of the *pl10R* mutant phenotypes by a wild-type DNAPol-ε but not by a T-C mutant DNA construct would finally confirm if the T444C mutation is indeed responsible for the *pl10R* mutation.

The enhanced sensitivity of *pl10R* mutant larvae to bleomycin, in terms of survival as well as double strand DNA breaks, further confirms this mutation to affect the DNApol-ε enzyme activity since this enzyme is known to be involved in DNA repair (Oshige *et al*., 2004; Pursel and Kunkel, 2008).

It is now generally believed that the DNApol-ε is one of the main replicative enzyme responsible for the leading strand synthesis (Pursell and Kunkel, 2008) and thus its defective functioning is expected to affect cell proliferation and growth. Growth and viability is reported to be affected in *Pol-ε* mutants in yeast (Morrison *et al*., 1990) although other reports suggest that the catalytic subunit of DNA polymerase-ε is not essential for cell viability in yeast (Kesti *et al*., 1999). However, this enzyme appears to have non-redundant role in *Xenopus* eggs (Shikata *et al*., 2006). In view of the fact that *DNApol-ε* mutation in *Drosophila* affects cell proliferation and endoreplication cycles in larval SGs and finally in death, this DNA polymerase appears to be essential in *Drosophila*.

The *pl10R* homozygotes, which are unlikely to produce any functional DNApol-ε because of the predicted premature chain termination (Fig. 6), presumably survive to larval stage because of the known maternal contribution of this essential replicative enzyme (Oshige *et al*., 2000; Yamaguchi *et al*., 1995). In the absence of an antibody that identifies the DNApol-ε of *Drosophila*, we could not estimate the enzyme levels in mutant larvae but we presume that as the maternal contribution of the DNApol-ε gets used up, the cells fail to divide or endoreplicate, generating the observed pleiotropic *pl10R* phenotypes. It is interesting that different larval tissues are affected to different degrees because of the non-availability of DNApol-ε in the *pl10R* mutants. Thus while imaginal discs and the imaginal cell clusters in larval gut and SG duct show very poor proliferation, the endoreplicating larval tissues respond differently. While the SG growth is severely stunted, the MTs and most of the endoreplicating gut cells appear nearly unaffected. These

differences may be due to a differential apportioning of the maternal DNApol-ε enzyme to different progenitor cells and to differences in the developmental replicative activity. The highly endoreplicated larval SGs are to some extent dispensable for development since larvae with very small SGs can also pupate and eclose as normal flies (Jones *et al*., 1998; personal observations). On the other hand, the gut and MTs are essential for larval life as well. Therefore, it appears that more of the maternally derived DNApol-ε enzyme may be apportioned to the gut and MT precursors than to the SG progenitors. Further, the SG cells undergo many more endoreplication cycles than the other larval endoreplicating tissues and, therefore, would suffer more because of the absence of an essential replicative enzyme.

It is interesting that the nucleoplasmic distribution of the omega speckles, visualized through the hsrω-n transcripts and Hrp36 protein, is affected in a manner reminiscent of stressed cells (Prasanth *et al*., 2000). The clustering of omega speckles in the *pl10R* mutant cells is not due to any typical cell stress since we find these cells to be completely free of the stress inducible Hsp70. In this context reports about the roles of DNApol-ε enzyme in chromatin remodeling (Pursel and Kunkel, 2008) on one hand and interactions between omega speckles and chromatin modeler like ISWI (Onorati *et al*., 2011) on the other may be interesting. The ISWI containing chromatin accessibility complex (CHRAC) of *Drosophila* includes DmCHRAC-14 (Corona *et al*., 2000), which is same as the DmPolε-p17 protein associated with DNApol-ε in its chromatin remodeling activity (Pursel and Kunkel, 2008). Further studies are needed to resolve this interesting interaction. In this context, it is interesting that the *pl10R* mutation is reported (Sengupta and Lakhotia, 2006) to dominantly enhance neurodegeneration in expanded polyQ-fly models. This effect may be due to the observed over-expression of the hsrω transcripts in *pl10R* mutant cells (Fig. 1) because the enhanced levels of these transcripts are known to enhance polyQ based neurodegeneration (Mallik and Lakhotia, 2009). Additionally, the *pl10R* allele may affect the chromatin remodeling role of DNApol-ε, which in turn can exaggerate the polyQ phenotype since compromised chromatin remodeling activity also enhances the polyQ damage (Mallik and Lakhotia, 2010). Further studies are needed to resolve these possibilities.

MATERIALS AND METHODS

Fly Genetics

Drosophila melanogaster cultures (wild type and mutants) were maintained at 24° ± 1°C on standard food containing agar, maize powder, yeast, and sugar. For cytological preparations, staged larvae were grown in Petri plates with food, supplemented with additional yeast for healthy growth. *Oregon* R^+ was used as wild-type strain. The various Exelixis deletion lines (Parks *et al*., 2004), listed in Supporting Information Table S1, *ru h th st cu sr e ca/TM6B* ("*rucuca*") and the *P*-element insertion mutant alleles $pnt^{KG04968}$, $P\{PZ\}pnt^{07825}$, $P(PZ)sec13^{01031}$, $RpS3^{Plac92}$, $P\{EPgy2\}ATPsyn\text{-}Cf6^{EY22484}$, $PBac\{WH\}CG6784^{f01032}$, and other stocks like *y w, hs-FLP; +; P{ry*$^+$*t7.2 = neo FRT}82B-Ubi-GFP*, *P{ry*$^+$*t7.2 = neo FRT}82B* and *Act-GAL4/CyO* were obtained from the Bloomington stock center. *Df(3R)M95A* (Hales and Fuller, 1997; Reuter *et al*., 1987) was obtained from Prof. Ruiz-Gomez, while the *CG4408-RNAi* and *DNApol-ε-RNAi* (*Pol-ε-RNAi*) transgenic lines were obtained from the NIG-Fly stock center (Japan).

The $l(3)pl10^R$ mutation was generated in our laboratory in the course of mobilization of the P-transposon insertion in the $hsr\omega^{05241}$ chromosome as a recessive late larval/pupal lethal mutation which was initially named as $hsr\omega^{pl10}$. To ascertain if the newly isolated $hsr\omega^{pl10}$. mutation was indeed an allele of *hsr*ω, the $hsr\omega^{pl10}/TM6B$ flies were crossed with ry^- flies and $hsr\omega^{pl10}/ry^-$ heterozygous progeny females were mated with *TM3, Sb,* $ry^-/TM6B$, *Tb* males. Progeny flies (red or rosy eyed and carrying the *TM3, Sb,* ry^- balancer) were individually back crossed to the parental $hsr\omega^{pl10}/TM6B$ flies and the resultant progeny homozygous for the *P*-insertion (red eyed due to ry^+ market in the P-transposon, nontubby, and nonstubbled bristle) and those without the P-transposon (rosy eyed and nonstubbled bristles) were checked for pupal lethality. These results established that the late larval/pupal lethal phenotype was independent of the *P-transposon* insertion in the *hsr*ω gene promoter, since several of the lines that did not carry the *P*-insertion showed the characteristic larval/pupal lethality and likewise, several of the lines that carried the *P*-insertion were normally viable. One line that showed recessive pupal lethality but did not carry the *P*-element was balanced with *TM6B* balancer and the mutation was renamed as $l(3)pl10^R$ (Sengupta, 2005).

Appropriate fly crosses were setup following standard methods to obtain progeny of desired genotypes.

Generation of $l(3)pl10^R$ Homozygous Somatic Clones in $l(3)pl10^R$/+ Background

The *y w; hs-FLP; P[ry*$^+$ *t7.2 = neoFRT]82B pl10R/ P[ry*$^+$*t7.2 = neoFRT]82B Ubi-GFP* $pl10R^+$ genotype was generated through appropriate crosses. First instar larvae were heat shocked for 1 h at 37°C and allowed to develop at 24°C to third instar larval stage. Imaginal discs (eye, leg, and wing) from these larvae were dissected out in Poels' salt solution (PSS, Tapadia and Lakhotia, 1997), fixed in 4% paraformaldehyde in phosphate buffered saline (PBS), stained with DAPI (1μg/

ml), washed in PBS, and finally mounted in DABCO for examination by confocal microscopy for presence of GFP-null (*pl10R* homozygous) and GFP-bright (+/+) clones in GFP-dull (*pl10R*/+) background.

Antibodies, Clones, and RNA Probes

Mouse monoclonal anti-Armadillo (dilution 1:20, gifted by Prof. Pradeep Sinha), mouse monoclonal anti-Wingless (dilution 1:30, Developmental Studies Hybridoma Bank, Iowa), mouse monoclonal mab22C10 antibody specific to neurons (dilution 1:100, Developmental Studies Hybridoma Bank, Iowa) were used for phenotypic characterization of the *pl10R* mutant larval tissues. Mouse monoclonal P11 (dilution 1:10, Saumweber *et al*., 1980) and rat monoclonal 7Fb (dilution 1:200, Velazquez and Lindquist, 1984) antibodies were used to detect the Hrp36 and heat induced Hsp70 proteins, respectively. Appropriate anti-mouse or anti-rat IgG secondary antibodies tagged with alkaline phosphatase (for colorimetric detection) or with AlexaFluor-488 (Molecular Probes) for fluorescent detection were used as described earlier (Lakhotia *et al*., 2001; Prasanth et al 2000).

Digoxigenein labeled anti-sense riboprobes were generated using *pDRM30* (Prasanth *et al*., 2000) for hsrω-n transcripts (Prasanth *et al*., 2000) and *SD09005* for the DNApol-ε transcripts (Drosophila Genomic Resource Center) using the Dig labeling kit from Roche (Germany). The *SD09005* clone contains about 2.25 kb of distal region of the *DNApol-ε* gene.

Partial Squash Preparation of Larval MTs for RNA:RNA In Situ Hybridization

MTs were dissected out in PSS from third instar larvae of different genotypes (see Results) and processed for preparation of partial squashes following Bendena *et al*. (1991). These were processed for RNA:RNA in situ hybridization as described earlier (Prasanth *et al*., 2000).

Whole Organ RNA:RNA In Situ Hybridization and Immunofluorescence Staining

The larval tissues from the desired genotypes were dissected out and were processed for RNA:RNA in situ hybridization and/or immune-staining as described by Prasanth *et al*. (2000). The hybridization and immunostaining signals were detected by confocal microscopy after staining with anti-DIG-rhodamine ab (Roche, Germany) and AlexaFluor-488 (Molecular Probes) anti-mouse secondary ab as described earlier (Prasanth *et al*., 2000).

Confocal images were obtained either with a Bio-Rad Radiance 2000 MP or Zeiss LSM 510 Meta confocal microscope.

PCR and Sequencing

Genomic DNAs from larvae of desired genotypes were isolated using standard SDS-Proteinase K lysis method followed by Phenol-Chloroform extraction (Sambrook and Russel, 2001). The DNAs were subjected to PCR with the various overlapping primer pairs (see Supporting Information Table S2 for details). PCR cycling parameters included initial denaturation at 94°C for 5 min followed by 35 cycles of 94°C for 45 sec, annealing for 30 sec (annealing temperatures for different primer pairs are noted in Supporting Information Table S2) and 72°C for 2 min 30 sec for amplicons more than 2.5 Kbp or 1 min 15 sec for amplicons less than 1.5 Kbp. Final extension was carried out at 72°C for 5 min. Amplicons were fractionated on 1% agarose gel with appropriate molecular markers. Subsequently the amplicons were eluted from the gel using silica beads as per manufacturer's instruction (Fermentas).

The eluted amplicons were processed for cycle sequencing as per manufacturer's (Applied Biosystems) instructions using ABI BigDye Terminator kit ver-1.1. DNA sequencing was performed on a 4-capillary automated DNA sequencer (Applied Biosystems 3130 Genetic Analyser platform). The sequences were analyzed by using Chromas Lite (Version-2.01) software. In silico analysis for alignment of the sequences and to identify variants, if any, was performed with Clustalw software (Thompson *et al*., 1994).

Semiquantitative RT-PCR

Total RNA was isolated from third instar larvae of the desired genotype (see Results) using TRIzol following the manufacturer's (Sigma-Aldrich, India) instructions. First strand c-DNA was synthesized using MMLV Reverse Transciptase (RT) as per manufacturer's instruction (Amersham). Briefly, 2 μg of RNA, 80 pM of oligo dT17 primer, 500 μM of dNTP mix, and 100 units of RT were added to the final 20 μl reaction volume. For PCR amplification, 1/10th volume of the RT-product was used. The different primer pairs used are listed in Table 2.

The thermal cycling parameters included initial denaturation at 94°C for 3 min followed by 27 cycles of 94°C for 30 sec, 60°C for 30 sec (except that in the case of DNApol-3F and DNApol-2R primer pairs annealing was carried out at 53°C), 72°C for 30 sec, finally extension at 72°C for 5 min. The PCR products were electrophoresed on 2% agarose gel.

Bleomycin Sensitivity Assay

Freshly hatched first instar larvae of the desired genotypes were transferred to standard *Drosophila* food mixed with bleomycin (concentration 2.5 or 5 μg/ml of food). For each genotype and treatment, three replicates with 75 first instar larvae were carried out. Number of third instar larvae and pupae in each plate were

Table 2
Primer Pairs Used for Determining the DNApol-ε Transcript Levels and its Splicing Through RT-PCR

S. No.	Primer name	Primer sequence (5′–3′)	Location
1	DNApol.3F	GTTCCGAGGATGCCACATTG	+718 to +737; exon3
2	DNApol.2R	CCACTGTCCACAAAAGATGCG	+845 to +825; exon3
3	DNApol-Int1.F	ATGTCCGACTCCAGCAAAGGC	+1 to +20; exon1
4	DNApol-Int1.R	TAGCCCGTCCGCTCCTGGC	+239 to +221; exon2
5	DNApol-Int2.F	CGAAATATGGCTTCGATCGGG	+191 to +211; exon2
6	DNApol-Int2.R	TAGGCCACCGTGCATTTGAA	+415 to +396; exon3
7	DNApol-Int3.F	TGCGACAGTCACATCATCAAC	+6,429 to +6,449; exon3
8	DNApol-Int3.R	TCTCATTTCGATCTCCTCGT	+6,654 to +6,635; exon4
9	G3PDH.F	CCACTGCCGAGGAGGTCAACTA	+3,438 to +3,459; exon5
10	G3PDH.R	GCTCAGGGTGATTGCGTATGCA	+3,646 to +3,625; exon6

Primers at serial no. 1, 2, 9, and 10 were used for RT-PCR shown in Figure 7 whereas primer pairs 3–4, 5–6, and 7–8 were used to check the splicing status of Pol-ε transcripts shown in Figure 9. Location of the primers 1–8 is given with respect to the *Pol-ε* gene whereas for 9 and 10 these are with respect to the *G3pdh* gene. F and R represent forward and reverse primers, respectively.

counted. Since bleomycin feeding caused some delay in development, the counting of third instar larvae and pupae was continued till day 7. Pupae were transferred to fresh food vials and the number of flies that eclosed in each vial were counted.

Bleomycin Treatment for DNA Damage Assay

Early third instar larvae (72 ± 2 h) of the desired genotype were transferred to normal *Drosophila* food supplemented with 50 mg/ml or 100 mg/ml of bleomycin for 48 h. Parallel control larvae were grown on the standard food.

Comet Assay

Single cell suspension was prepared from imaginal discs dissected out from control and treated larvae as described by Siddique *et al*. (2005). Cell viability was measured by trypan blue staining after Phillips (1973). Alkaline comet assay was performed following Siddique *et al*. (2005). Briefly, the single cell suspension was mixed with low melting agarose to a final concentration of 0.75%. The cell suspension was spread on the slides precoated with 1% normal melting agarose and allowed to solidify under a coverslip at 4°C. After solidification, coverslips were removed and the slides were incubated in lysis buffer (2.5 M NaCl, 100 mM EDTA, 10 mM Trizma base, 1% TritonX-100, 10% DMSO, pH 10) for 2 h at 4°C followed by electrophoresis and subsequent staining with propidium iodide (1 μg/ml). The slides were observed under Nikon Ti90 fluorescence microscope and the comets were analyzed using the TriTek CometScore™ Freeware v.15 (available at: http://www.autocomet.com/products_cometscore.php).

All images were assembled with Adobe Photoshop 7.0.

ACKNOWLEDGMENTS

The authors acknowledge the Bloomington *Drosophila* Stock Centre (USA), the NIG-FLY Stock Center (Japan) and Prof. Ruiz-Gomez for fly stocks. The authors thank Prof. H. Saumweber and Prof. M. B. Evgen'ev for the P11 and 7Fb antibodies, respectively. Support for the Confocal Microscope facility by the DST is also acknowledged.

NOTE ADDED IN PROOF

In a recent publication, Brooks *et al*. (Brooks AN, Aspden JL, Podgornaia AI, Rio DC and Brenner SE. 2011. Identification and experimental validation of splicing regulatory elements in *Drosophila melanogaster* reveals functionally conserved splicing enhancers in metazoans. *RNA* published online August 24, 2011 DOI: 10.1261/rna.2696311) identified TAAATT as one of the 5′ intronic splice enhancer for transcripts with short exons and short introns. It is significant that the T444C base substitution in the *pl10R* allele identified in our study changes TAAATT motif (+444 to +449) to CAAATT and since the concerned exon and the intron of the *DNA-pol-e* gene are short, it is possible that the T444C change may indeed be responsible for our finding that the intron 1 is not spliced out in the *pl10R* mutants.

LITERATURE CITED

Akanksha, Mallik M, Roshan FB, Lakhotia SC. 2008. The *hsrω*^{05241} allele of the non-coding *hsrω* gene of *Drosophila melanogaster* is not responsible for male sterility as reported earlier. J Genet 87:87–90.

Aoyagi N, Oshige M, Horose F, Kuroda K, Matsukage A, Sakaguchi K. 1997. DNA polymerase from *Drosophila melanogaster*. Biochem Biophys Res Commun 230:297–301.

Araki H, Ropp PA, Johnson AL, Johnston LH, Morrison A, Sugino A. 1992. DNA polymerase II, the probable homolog of mammalian DNA polymerase epsilon, replicates chromosomal DNA in the yeast *Saccharomyces cerevisiae*. EMBO J 11:733–740.

Bendena WG, Ayme-Southgate A, Garbe JC, Pardu ML. 1991. Expression of heat-shock locus *hsr-omega* in

non-stressed cells during development in *Drosophila melanogaster*. Dev Biol 144:65–77.

Budd ME, Campbell JL. 1993. DNA polymerases delta and epsilon are required for chromosomal replication in *Saccharomyces cerevisiae*. Mol Cell Biol 13:496–505.

Chen Y, Stephan W. 2003. Compensatory evolution of a precursor messenger RNA secondary structure in the *Drosophila melanogaster Adh* gene. Proc Natl Acad Sci USA 100:11499–11504.

Corona ,DFV, Eberharter A, Budde A, Deuring R, Ferrari S, Varga-Weisz P, Wilm M, Tamkun J, Becker PB. 2000. Two histone fold proteins, CHRAC-14 and CHRAC-16, are developmentally regulated subunits of chromatin accessibility complex (CHRAC). EMBO J19:3049–3059.

Drysdale RA, Crosby MA; The Flybase Consortium. 2005. Flybase: Genes and gene models. Nucleic Acids Res 33:D390–D395.

Fujita SC, Zipursky SL, Benzer S, Ferrus A, Shotwell SL. 1982. Monoclonal antibodies against the *Drosophila* nervous system. Proc Natl Acad Sci USA 79:7929–7933.

Golic KG, Lindquist S. 1989. The FLP recombinase of yeast catalyzes site-specific recombination in the *Drosophila* genome. Cell 59:499–509.

Hales KG, Fuller MT. 1997. Developmentally regulated mitochondrial fusion mediated by a conserved, novel, predicted GTPase. Cell 90:121–129.

Jones NA, Kuo YM, Sun YH, Beckendorf SK. 1998. The *Drosophila pax* gene eye gone is required for embryonic salivary duct development. Development 125:4163–4174.

Kesti T, Flick K, Keranen S, Syvaoja JE, Wittenberg C. 1999. DNA polymerase epsilon catalytic domains are dispensable for DNA replication, DNA repair, and cell viability. Mol Cell 3:679–685.

Kreahling JM, Graveley BR. 2005. The iStem, a long-range RNA secondary structure element required for efficient exon inclusion in the *Drosophila* Dscam pre-mRNA. Mol Cell Biol 25:10251–10260.

Kumaravel TS, Jha AN. 2006. Reliable Comet assay measurements for detecting DNA damage induced by ionising radiation and chemicals. Mutat Res 605:7–16.

Lakhotia SC, Rajendra TK, Prasanth KV. 2001. Developmental regulation and complex organization of the promoter of the noncoding *hsr*ω gene of *Drosophila melanogaster*. J Biosci 26:25–38.

Lakhotia SC, Ray P, Rajendra TK, Prasanth KV. 1999. The non-coding transcripts of *hsr-omega* gene in *Drosophila*: Do they regulate trafficking and availability of nuclear RNA processing factors? Curr Sci 77:553–563.

Lindsley DL, Zimm GG. 1992. The genome of *Drosophila melanogaster*. San Diego, CA: Academic Press Inc.

Loeb DD, Mack AA, Tian R. 2002. A secondary structure that contains the 5′ and 3′ splice sites suppresses splicing of duck hepatitis B virus pregenomic RNA. J Virol 76:10195–10202.

Mallik M, Lakhotia SC. 2009. RNAi for the large non-coding hsrω transcripts suppresses polyglutamine pathogenesis in *Drosophila* models. RNA Biol 6:464–478.

Mallik M, Lakhotia SC. 2010. Modifiers and mechanisms of multi-system polyglutamine neurodegenerative disorders: Lessons from fly models. J. Genetics 89:497–526

Morrison A, Araki H, Clark AB, Hamatake RK, Sugino A. 1990. A third essential DNA polymerase in *S. cerevisiae*. Cell 62:1143–1151.

Nishida C, Reinhard P, Linn S. 1988. DNA repair synthesis in human fibroblast requires DNA polymerase delta. J Biol Chem 263:501–510.

Olive PL. 1999. DNA damage and repair in individual cells: Applications of the Comet assay in radiobiology. Int J Radiat Biol 75:395–405.

Onorati MC, Lazzaro S, Mallik M, Ingrassia AMR, Singh AK, Chaturvedi DP, Lakhotia SC, Corona DFV. 2011. The ISWI chromatin remodeler organizes the hsrω ncRNA-containing omega speckle nuclear compartments. PLoS Genet 7:e1002096.

Oshige M, Yoshida H, Hirose F, Takata KI, Inoue Y, Aoyagi N, Yamaguchi M, Koiwai O, Matsukage A, and Sakaguchi K. 2000. Molecular cloning and expression during development of the *Drosophila* gene for the catalytic subunit of DNA polymerase epsilon. Gene 256:93–100.

Oshige M, Takeuchi R, Ruike R, Kuroda K, Sakaguchia K. 2004. Subunit protein-affinity isolation of *Drosophila* DNA polymerase ε catalytic subunit. Protein Expr Purif 35:248–256.

Parks AL, Cook KR, Belvin M, Dompe NA, Fawcett R, Huppert K, Tan LR, Winter CG, Bogart KP, Deal JE, Deal-Herr ME, Grant D, Marcinko M, Miyazaki WY, Robertson S, Shaw KJ, Tabios M, Vysotskaia V, Zhao L, Andrade RS, Edgar KA, Howie E, Killpack K, Milash B, Norton A, Thao D, Whittaker K, Winner MA, Friedman L, Margolis J, Singer MA, Kopczynski C, Curtis D, Kaufman TC, Plowman GD, Duyk G, Francis-Lang HL. 2004. Systematic generation of high-resolution deletion coverage of the Drosophila genome. Nat Genet 36:288–292.

Phillips HJ. 1973. Dye exclusion tests for cell viability. In: Kruse PF Jr, Patterson MK Jr, editors. Tissue culture methods and applications. New York: Academic Press. pp 406–408.

Povirk LF, Wü bker W, Köhnlein W, Hutchinson F. 1977. DNA double-strand breaks and alkali-labile bonds produced by bleomycin. Nucleic Acids Res 4:3573–3580.

Povirk LF, Han YH, Steighner RJ. 1989. Structure of bleomycin-induced DNA double-strand breaks: Predominance of blunt ends and single-base 50 extensions. Biochemistry 28:5808–5814.

Prasanth KV, Rajendra TK, Lal AK, Lakhotia SC. 2000. Omega speckles—A novel class of nuclear speckles containing hnRNPs associated with noncoding hsr-omega RNA in *Drosophila*. J Cell Sci 113:3485–3497.

Pursell ZF, Kunkel TA. 2008. DNA polymerase−ε: A polymerase of unusual size (and complexity). Prog Nucleic Acid Res Mol Biol 82:101–145.

Rajendra TK, Prasanth KV, Lakhotia SC. 2001. Male sterility associated with over-expression of the noncoding *hsr*ω gene in cyst cells of testis of *Drosophila melanogaster*. J Genet 80:97–110.

Reuter G, Gausz J, Gyurkovics H, Friede B, Bang R, Spierer A, Hall LM, Spierer P. 1987. Modifiers of position—Effect variegation in the region from 86C to 88B of the *Drosophila melanogaster* third chromosome. Mol Gen Genet 210:429–436.

Riggleman B, Schedl P, Wieschaus E. 1990. Spatial expression of the Drosophila segment polarity gene armadillo is posttranscriptionally regulated by wingless. Cell 63:549–560.

Sambrook J, Russel DW. 2001. Molecular cloning: A laboratory manual. Cold Spring Harbor, NY: Cold Spring Harbor Laboratory Press.

Saumweber H, Symmons P, Kabisch R, Will H, Bonhoeffer F. 1980. Monoclonal antibodies against chromosomal proteins of *Drosophila melanogaster*. Chromosoma 80:253–275.

Sengupta S. 2005.Studies on a novel gene interacting with *hsr*ω gene and their roles as modifiers in polyglutamine induced neurodegeneration in *Drosophila melanogaster*. PhD Thesis. Varanasi: Banaras Hindu University.

Sengupta S, Lakhotia SC. 2006. Altered expressions of the noncoding *hsr-omega* gene enhances poly-Q-induced neurotoxicity in *Drosophila*. RNA Biol 3:28–35.

Shikata K, Sasa-Masuda T, Okuno Y, Waga S, Sugino A. 2006. The DNA polymerase activity of Pol ε holoenzyme is required for rapid and efficient chromosomal DNA replication in Xenopus egg extracts. BMC Biochemi 7:21.

Siddique HR, Chowdhuri DK, Saxena DK, Dhawan A. 2005. Validation of *Drosophila melanogaster* as an in vivo model for genotoxicity assessment using modified alkaline Comet assay. Mutagenesis 20:285–290.

Tapadia M, Lakhotia SC. 1997. Specific induction of the *hsr*ω locus of *Drosophila melanogaster* by amides. Chromosome Res 5:1–4.

Thompson JD, Desmond G, Higgins, Toby J. Gibson. 1994. CLUSTAL W: Improving the sensitivity of progressive multiple sequence alignment through sequence weighting, position-specific gap penalties and weight matrix choice. Nucleic Acids Res 22:4673–4680.

Velazquez JM, Lindquist S. 1984. hsp70: Nuclear concentration during environmental stress and cytoplasmic storage during recovery. Cell 36:655–662.

Warf MB, Berglund JA. 2010. The role of RNA structure in regulating pre-mRNA splicing. Trends Biochem Sci 35:169–178.

Xu T, Rubin GM. 1993. Analysis of genetic mosaics in developing and adult *Drosophila* tissues. Development 117:1223–1237.

Yamaguchi M, Hirose F, Nishimoto Y, Naruge T, Ikeda M, Hachiya T, Tamai K, Kuroda K, Matsukage A. 1995. Expression patterns of DNA replication enzymes and the regulatory factor DREF during *Drosophila* development analyzed with specific antibodies. Biol Cell 85:147–155.

Zlotkin T, Kaufmann G, Jiang Y, Lee MY, Uitto L, Syväoja J, Dornreiter I, Fanning E, Nethanel T. 1996. DNA polymerase epsilon may be dispensable for SV40- but not cellular-DNA replication. EMBO J 15:2298–2305.